



Measurements of indirect CP asymmetries in $D^0 \rightarrow K^- K^+$ and $D^0 \rightarrow \pi^- \pi^+$ decays

The LHCb collaboration[†]

Abstract

A study of indirect CP violation in D^0 mesons through the determination of the parameter A_Γ is presented using a data sample of pp collisions, corresponding to an integrated luminosity of 1.0 fb^{-1} , collected with the LHCb detector and recorded at the centre-of-mass energy of 7 TeV at the LHC. The parameter A_Γ is the asymmetry of the effective lifetimes measured in decays of D^0 and \bar{D}^0 mesons to the CP eigenstates $K^- K^+$ and $\pi^- \pi^+$. Fits to the data sample yield $A_\Gamma(KK) = (-0.35 \pm 0.62 \pm 0.12) \times 10^{-3}$ and $A_\Gamma(\pi\pi) = (0.33 \pm 1.06 \pm 0.14) \times 10^{-3}$, where the first uncertainties are statistical and the second systematic. The results represent the world's best measurements of these quantities. They show no difference in A_Γ between the two final states and no indication of CP violation.

Submitted to Phys. Rev. Lett.

[†] Authors are listed on the following pages.

LHCb collaboration

R. Aaij⁴⁰, B. Adeva³⁶, M. Adinolfi⁴⁵, C. Adrover⁶, A. Affolder⁵¹, Z. Ajaltouni⁵, J. Albrecht⁹, F. Alessio³⁷, M. Alexander⁵⁰, S. Ali⁴⁰, G. Alkhazov²⁹, P. Alvarez Cartelle³⁶, A.A. Alves Jr²⁴, S. Amato², S. Amerio²¹, Y. Amhis⁷, L. Anderlini^{17,f}, J. Anderson³⁹, R. Andreassen⁵⁶, J.E. Andrews⁵⁷, R.B. Appleby⁵³, O. Aquines Gutierrez¹⁰, F. Archilli¹⁸, A. Artamonov³⁴, M. Artuso⁵⁸, E. Aslanides⁶, G. Auriemma^{24,m}, M. Baalouch⁵, S. Bachmann¹¹, J.J. Back⁴⁷, A. Badalov³⁵, C. Baesso⁵⁹, V. Balagura³⁰, W. Baldini¹⁶, R.J. Barlow⁵³, C. Barschel³⁷, S. Barsuk⁷, W. Barter⁴⁶, Th. Bauer⁴⁰, A. Bay³⁸, J. Beddow⁵⁰, F. Bedeschi²², I. Bediaga¹, S. Belogurov³⁰, K. Belous³⁴, I. Belyaev³⁰, E. Ben-Haim⁸, G. Bencivenni¹⁸, S. Benson⁴⁹, J. Benton⁴⁵, A. Berezhtoy³¹, R. Bernet³⁹, M.-O. Bettler⁴⁶, M. van Beuzekom⁴⁰, A. Bien¹¹, S. Bifani⁴⁴, T. Bird⁵³, A. Bizzeti^{17,h}, P.M. Bjørnstad⁵³, T. Blake³⁷, F. Blanc³⁸, J. Blouw¹⁰, S. Blusk⁵⁸, V. Bocci²⁴, A. Bondar³³, N. Bondar²⁹, W. Bonivento¹⁵, S. Borghi⁵³, A. Borgia⁵⁸, T.J.V. Bowcock⁵¹, E. Bowen³⁹, C. Bozzi¹⁶, T. Brambach⁹, J. van den Brand⁴¹, J. Bressieux³⁸, D. Brett⁵³, M. Britsch¹⁰, T. Britton⁵⁸, N.H. Brook⁴⁵, H. Brown⁵¹, A. Bursche³⁹, G. Busetto^{21,q}, J. Buytaert³⁷, S. Cadeddu¹⁵, O. Callot⁷, M. Calvi^{20,j}, M. Calvo Gomez^{35,n}, A. Camboni³⁵, P. Campana^{18,37}, D. Campora Perez³⁷, A. Carbone^{14,c}, G. Carboni^{23,k}, R. Cardinale^{19,i}, A. Cardini¹⁵, H. Carranza-Mejia⁴⁹, L. Carson⁵², K. Carvalho Akiba², G. Casse⁵¹, L. Castillo Garcia³⁷, M. Cattaneo³⁷, Ch. Cauet⁹, R. Cenci⁵⁷, M. Charles⁵⁴, Ph. Charpentier³⁷, S.-F. Cheung⁵⁴, N. Chiapolini³⁹, M. Chrzasczcz^{39,25}, K. Ciba³⁷, X. Cid Vidal³⁷, G. Ciezarek⁵², P.E.L. Clarke⁴⁹, M. Clemencic³⁷, H.V. Cliff⁴⁶, J. Closier³⁷, C. Coca²⁸, V. Coco⁴⁰, J. Cogan⁶, E. Cogneras⁵, P. Collins³⁷, A. Comerma-Montells³⁵, A. Contu^{15,37}, A. Cook⁴⁵, M. Coombes⁴⁵, S. Coquereau⁸, G. Corti³⁷, B. Couturier³⁷, G.A. Cowan⁴⁹, D.C. Craik⁴⁷, M. Cruz Torres⁵⁹, S. Cunliffe⁵², R. Currie⁴⁹, C. D'Ambrosio³⁷, P. David⁸, P.N.Y. David⁴⁰, A. Davis⁵⁶, I. De Bonis⁴, K. De Bruyn⁴⁰, S. De Capua⁵³, M. De Cian¹¹, J.M. De Miranda¹, L. De Paula², W. De Silva⁵⁶, P. De Simone¹⁸, D. Decamp⁴, M. Deckenhoff⁹, L. Del Buono⁸, N. Deléage⁴, D. Derkach⁵⁴, O. Deschamps⁵, F. Dettori⁴¹, A. Di Canto¹¹, H. Dijkstra³⁷, M. Dogaru²⁸, S. Donleavy⁵¹, F. Dordei¹¹, A. Dosil Suárez³⁶, D. Dosselt⁴⁷, A. Dovbnya⁴², F. Dupertuis³⁸, P. Durante³⁷, R. Dzhelezhadina³⁴, A. Dziurda²⁵, A. Dzyuba²⁹, S. Easo⁴⁸, U. Egede⁵², V. Egorychev³⁰, S. Eidelman³³, D. van Eijk⁴⁰, S. Eisenhardt⁴⁹, U. Eitschberger⁹, R. Ekelhof⁹, L. Eklund^{50,37}, I. El Rifai⁵, Ch. Elsasser³⁹, A. Falabella^{14,e}, C. Färber¹¹, C. Farinelli⁴⁰, S. Farrar⁵¹, D. Ferguson⁴⁹, V. Fernandez Albor³⁶, F. Ferreira Rodrigues¹, M. Ferro-Luzzi³⁷, S. Filippov³², M. Fiore^{16,e}, C. Fitzpatrick³⁷, M. Fontana¹⁰, F. Fontanelli^{19,i}, R. Forty³⁷, O. Francisco², M. Frank³⁷, C. Frei³⁷, M. Frosini^{17,37,f}, E. Furfaro^{23,k}, A. Gallas Torreira³⁶, D. Galli^{14,c}, M. Gandelman², P. Gandini⁵⁸, Y. Gao³, J. Garofoli⁵⁸, P. Garosi⁵³, J. Garra Tico⁴⁶, L. Garrido³⁵, C. Gaspar³⁷, R. Gauld⁵⁴, E. Gersabeck¹¹, M. Gersabeck⁵³, T. Gershon⁴⁷, Ph. Ghez⁴, V. Gibson⁴⁶, L. Giubega²⁸, V.V. Gligorov³⁷, C. Göbel⁵⁹, D. Golubkov³⁰, A. Golutvin^{52,30,37}, A. Gomes², P. Gorbounov^{30,37}, H. Gordon³⁷, M. Grabalosa Gándara⁵, R. Graciani Diaz³⁵, L.A. Granado Cardoso³⁷, E. Graugés³⁵, G. Graziani¹⁷, A. Grecu²⁸, E. Greening⁵⁴, S. Gregson⁴⁶, P. Griffith⁴⁴, L. Grillo¹¹, O. Grünberg⁶⁰, B. Gui⁵⁸, E. Gushchin³², Yu. Guz^{34,37}, T. Gys³⁷, C. Hadjivasiliou⁵⁸, G. Haefeli³⁸, C. Haen³⁷, S.C. Haines⁵³, S. Hall⁵², B. Hamilton⁵⁷, T. Hampson⁴⁵, S. Hansmann-Menzemer¹¹, N. Harnew⁵⁴, S.T. Harnew⁴⁵, J. Harrison⁵³, T. Hartmann⁶⁰, J. He³⁷, T. Head³⁷, V. Heijne⁴⁰, K. Hennessy⁵¹, P. Henrard⁵, J.A. Hernandez Morata³⁶, E. van Herwijnen³⁷, M. Heß⁶⁰, A. Hicheur¹, E. Hicks⁵¹, D. Hill⁵⁴, M. Hoballah⁵, C. Hombach⁵³, W. Hulsbergen⁴⁰, P. Hunt⁵⁴, T. Huse⁵¹, N. Hussain⁵⁴, D. Hutchcroft⁵¹, D. Hynds⁵⁰, V. Iakovenko⁴³, M. Idzik²⁶, P. Ilten¹², R. Jacobsson³⁷, A. Jaeger¹¹, E. Jans⁴⁰, P. Jaton³⁸, A. Jawahery⁵⁷, F. Jing³, M. John⁵⁴, D. Johnson⁵⁴, C.R. Jones⁴⁶, C. Joram³⁷, B. Jost³⁷, M. Kaballo⁹, S. Kandybei⁴², W. Kanso⁶, M. Karacson³⁷, T.M. Karbach³⁷, I.R. Kenyon⁴⁴, T. Ketel⁴¹, B. Khanji²⁰, O. Kochebina⁷, I. Komarov³⁸, R.F. Koopman⁴¹, P. Koppenburg⁴⁰, M. Korolev³¹, A. Kozlinskiy⁴⁰, L. Kravchuk³², K. Kreplin¹¹, M. Kreps⁴⁷, G. Krocker¹¹, P. Krokovny³³, F. Kruse⁹, M. Kucharczyk^{20,25,37,j}, V. Kudryavtsev³³, K. Kurek²⁷, T. Kvaratskheliya^{30,37}, V.N. La Thi³⁸, D. Lacarrere³⁷, G. Lafferty⁵³, A. Lai¹⁵, D. Lambert⁴⁹, R.W. Lambert⁴¹, E. Lanciotti³⁷, G. Lanfranchi¹⁸, C. Langenbruch³⁷, T. Latham⁴⁷, C. Lazzeroni⁴⁴, R. Le Gac⁶, J. van Leerdam⁴⁰, J.-P. Lees⁴, R. Lefèvre⁵, A. Leflat³¹, J. Lefrançois⁷, S. Leo²², O. Leroy⁶, T. Lesiak²⁵, B. Leverington¹¹, Y. Li³, L. Li Gioi⁵, M. Liles⁵¹, R. Lindner³⁷, C. Linn¹¹, B. Liu³, G. Liu³⁷, S. Lohn³⁷, I. Longstaff⁵⁰, J.H. Lopes², N. Lopez-March³⁸, H. Lu³, D. Lucchesi^{21,q}, J. Luisier³⁸, H. Luo⁴⁹, O. Lupton⁵⁴, F. Machefert⁷, I.V. Machikhiliyan³⁰, F. Maciuc²⁸, O. Maev^{29,37}, S. Malde⁵⁴, G. Manca^{15,d}, G. Mancinelli⁶, J. Maratas⁵, U. Marconi¹⁴, P. Marino^{22,s}, R. Märki³⁸, J. Marks¹¹, G. Martellotti²⁴, A. Martens⁸, A. Martín Sánchez⁷, M. Martinelli⁴⁰, D. Martinez Santos^{41,37}, D. Martins Tostes², A. Martynov³¹, A. Massafferri¹, R. Matev³⁷, Z. Mathe³⁷, C. Matteuzzi²⁰, E. Maurice⁶, A. Mazurov^{16,37,e}, J. McCarthy⁴⁴, A. McNab⁵³, R. McNulty¹², B. McKelley⁵¹, B. Meadows^{56,54}, F. Meier⁹, M. Meissner¹¹, M. Merk⁴⁰, D.A. Milanes⁸, M.-N. Minard⁴, J. Molina Rodriguez⁵⁹, S. Monteil⁵, D. Moran⁵³, P. Morawski²⁵, A. Mordà⁶, M.J. Morello^{22,s}, R. Mountain⁵⁸, I. Mous⁴⁰, F. Muheim⁴⁹, K. Müller³⁹, R. Muresan²⁸, B. Muryn²⁶, B. Muster³⁸, P. Naik⁴⁵, T. Nakada³⁸, R. Nandakumar⁴⁸, I. Nasteva¹, M. Needham⁴⁹, S. Neubert³⁷, N. Neufeld³⁷, A.D. Nguyen³⁸, T.D. Nguyen³⁸, C. Nguyen-Mau^{38,o}, M. Nicol⁷, V. Niess⁵, R. Niet⁹, N. Nikitin³¹, T. Nikodem¹¹, A. Nomerotski⁵⁴, A. Novoselov³⁴, A. Oblakowska-Mucha²⁶, V. Obraztsov³⁴, S. Oggero⁴⁰, S. Ogilvy⁵⁰, O. Okhrimenko⁴³, R. Oldeman^{15,d}, M. Orlandea²⁸, J.M. Otalora Goicochea², P. Owen⁵², A. Oyanguren³⁵, B.K. Pal⁵⁸, A. Palano^{13,b}, M. Palutan¹⁸, J. Panman³⁷, A. Papanestis⁴⁸, M. Pappagallo⁵⁰, C. Parkes⁵³, C.J. Parkinson⁵², G. Passaleva¹⁷, G.D. Patel⁵¹, M. Patel⁵², G.N. Patrick⁴⁸, C. Patrignani^{19,i}, C. Pavel-Nicorescu²⁸, A. Pazos Alvarez³⁶, A. Pearce⁵³, A. Pellegrino⁴⁰, G. Penso^{24,l}, M. Pepe Altarelli³⁷, S. Perazzini^{14,c}, E. Perez Trigo³⁶, A. Pérez-Calero Yzquierdo³⁵, P. Perret⁵, M. Perrin-Terrin⁶,

L. Pescatore⁴⁴, E. Pesen⁶¹, G. Pessina²⁰, K. Petridis⁵², A. Petrolini^{19,i}, A. Phan⁵⁸, E. Picatoste Olloqui³⁵, B. Pietrzyk⁴, T. Pilar⁴⁷, D. Pinci²⁴, S. Playfer⁴⁹, M. Plo Casasus³⁶, F. Polci⁸, G. Polok²⁵, A. Poluektov^{47,33}, E. Polycarpo², A. Popov³⁴, D. Popov¹⁰, B. Popovici²⁸, C. Potterat³⁵, A. Powell⁵⁴, J. Prisciandaro³⁸, A. Pritchard⁵¹, C. Prouve⁷, V. Pugatch⁴³, A. Puig Navarro³⁸, G. Punzi^{22,r}, W. Qian⁴, B. Rachwal²⁵, J.H. Rademacker⁴⁵, B. Rakotomiaramanana³⁸, M.S. Rangel², I. Raniuk⁴², N. Rauschmayr³⁷, G. Raven⁴¹, S. Redford⁵⁴, S. Reichert⁵³, M.M. Reid⁴⁷, A.C. dos Reis¹, S. Ricciardi⁴⁸, A. Richards⁵², K. Rinnert⁵¹, V. Rives Molina³⁵, D.A. Roa Romero⁵, P. Robbe⁷, D.A. Roberts⁵⁷, A.B. Rodrigues¹, E. Rodrigues⁵³, P. Rodriguez Perez³⁶, S. Roiser³⁷, V. Romanovsky³⁴, A. Romero Vidal³⁶, M. Rotondo²¹, J. Rouvinet³⁸, T. Ruf³⁷, F. Ruffini²², H. Ruiz³⁵, P. Ruiz Valls³⁵, G. Sabatino^{24,k}, J.J. Saborido Silva³⁶, N. Sagidova²⁹, P. Sail⁵⁰, B. Saitta^{15,d}, V. Salustino Guimaraes², B. Sanmartin Sedes³⁶, R. Santacesaria²⁴, C. Santamarina Rios³⁶, E. Santovetti^{23,k}, M. Sapunov⁶, A. Sarti¹⁸, C. Satriano^{24,m}, A. Satta²³, M. Savrie^{16,e}, D. Savrina^{30,31}, M. Schiller⁴¹, H. Schindler³⁷, M. Schlupp⁹, M. Schmelling¹⁰, B. Schmidt³⁷, O. Schneider³⁸, A. Schopper³⁷, M.-H. Schune⁷, R. Schwemmer³⁷, B. Sciascia¹⁸, A. Sciubba²⁴, M. Seco³⁶, A. Semennikov³⁰, K. Senderowska²⁶, I. Sepp⁵², N. Serra³⁹, J. Serrano⁶, P. Seyfert¹¹, M. Shapkin³⁴, I. Shapoval^{16,42,e}, Y. Shcheglov²⁹, T. Shears⁵¹, L. Shekhtman³³, O. Shevchenko⁴², V. Shevchenko³⁰, A. Shires⁹, R. Silva Coutinho⁴⁷, M. Sirendi⁴⁶, N. Skidmore⁴⁵, T. Skwarnicki⁵⁸, N.A. Smith⁵¹, E. Smith^{54,48}, E. Smith⁵², J. Smith⁴⁶, M. Smith⁵³, M.D. Sokoloff⁵⁶, F.J.P. Soler⁵⁰, F. Soomro³⁸, D. Souza⁴⁵, B. Souza De Paula², B. Spaan⁹, A. Sparkes⁴⁹, P. Spradlin⁵⁰, F. Stagni³⁷, S. Stahl¹¹, O. Steinkamp³⁹, S. Stevenson⁵⁴, S. Stoica²⁸, S. Stone⁵⁸, B. Storaci³⁹, M. Straticiu²⁸, U. Straumann³⁹, V.K. Subbiah³⁷, L. Sun⁵⁶, W. Sutcliffe⁵², S. Swientek⁹, V. Syropoulos⁴¹, M. Szczekowski²⁷, P. Szczypka^{38,37}, D. Szilard², T. Szumlak²⁶, S. T'Jampens⁴, M. Teklishyn⁷, E. Teodorescu²⁸, F. Teubert³⁷, C. Thomas⁵⁴, E. Thomas³⁷, J. van Tilburg¹¹, V. Tisserand⁴, M. Tobin³⁸, S. Tolk⁴¹, D. Tonelli³⁷, S. Topp-Joergensen⁵⁴, N. Torr⁵⁴, E. Tournefier^{4,52}, S. Tourneur³⁸, M.T. Tran³⁸, M. Tresch³⁹, A. Tsaregorodtsev⁶, P. Tsopelas⁴⁰, N. Tuning^{40,37}, M. Ubeda Garcia³⁷, A. Ukleja²⁷, A. Ustyuzhanin^{52,p}, U. Uwer¹¹, V. Vagnoni¹⁴, G. Valenti¹⁴, A. Vallier⁷, R. Vazquez Gomez¹⁸, P. Vazquez Regueiro³⁶, C. Vázquez Sierra³⁶, S. Vecchi¹⁶, J.J. Velthuis⁴⁵, M. Veltri^{17,g}, G. Veneziano³⁸, M. Vesterinen³⁷, B. Viaud⁷, D. Vieira², X. Vilasis-Cardona^{35,n}, A. Vollhardt³⁹, D. Volyanskyy¹⁰, D. Voong⁴⁵, A. Vorobyev²⁹, V. Vorobyev³³, C. Voß⁶⁰, H. Voss¹⁰, R. Waldi⁶⁰, C. Wallace⁴⁷, R. Wallace¹², S. Wandernoth¹¹, J. Wang⁵⁸, D.R. Ward⁴⁶, N.K. Watson⁴⁴, A.D. Webber⁵³, D. Websdale⁵², M. Whitehead⁴⁷, J. Wicht³⁷, J. Wiechczynski²⁵, D. Wiedner¹¹, L. Wiggers⁴⁰, G. Wilkinson⁵⁴, M.P. Williams^{47,48}, M. Williams⁵⁵, F.F. Wilson⁴⁸, J. Wimberley⁵⁷, J. Wishahi⁹, W. Wislicki²⁷, M. Witek²⁵, G. Wormser⁷, S.A. Wotton⁴⁶, S. Wright⁴⁶, S. Wu³, K. Wyllie³⁷, Y. Xie^{49,37}, Z. Xing⁵⁸, Z. Yang³, X. Yuan³, O. Yushchenko³⁴, M. Zangoli¹⁴, M. Zavertyaev^{10,a}, F. Zhang³, L. Zhang⁵⁸, W.C. Zhang¹², Y. Zhang³, A. Zhelezov¹¹, A. Zhokhov³⁰, L. Zhong³, A. Zvyagin³⁷.

¹ Centro Brasileiro de Pesquisas Físicas (CBPF), Rio de Janeiro, Brazil

² Universidade Federal do Rio de Janeiro (UFRJ), Rio de Janeiro, Brazil

³ Center for High Energy Physics, Tsinghua University, Beijing, China

⁴ LAPP, Université de Savoie, CNRS/IN2P3, Annecy-Le-Vieux, France

⁵ Clermont Université, Université Blaise Pascal, CNRS/IN2P3, LPC, Clermont-Ferrand, France

⁶ CPPM, Aix-Marseille Université, CNRS/IN2P3, Marseille, France

⁷ LAL, Université Paris-Sud, CNRS/IN2P3, Orsay, France

⁸ LPNHE, Université Pierre et Marie Curie, Université Paris Diderot, CNRS/IN2P3, Paris, France

⁹ Fakultät Physik, Technische Universität Dortmund, Dortmund, Germany

¹⁰ Max-Planck-Institut für Kernphysik (MPIK), Heidelberg, Germany

¹¹ Physikalisches Institut, Ruprecht-Karls-Universität Heidelberg, Heidelberg, Germany

¹² School of Physics, University College Dublin, Dublin, Ireland

¹³ Sezione INFN di Bari, Bari, Italy

¹⁴ Sezione INFN di Bologna, Bologna, Italy

¹⁵ Sezione INFN di Cagliari, Cagliari, Italy

¹⁶ Sezione INFN di Ferrara, Ferrara, Italy

¹⁷ Sezione INFN di Firenze, Firenze, Italy

¹⁸ Laboratori Nazionali dell'INFN di Frascati, Frascati, Italy

¹⁹ Sezione INFN di Genova, Genova, Italy

²⁰ Sezione INFN di Milano Bicocca, Milano, Italy

²¹ Sezione INFN di Padova, Padova, Italy

²² Sezione INFN di Pisa, Pisa, Italy

²³ Sezione INFN di Roma Tor Vergata, Roma, Italy

²⁴ Sezione INFN di Roma La Sapienza, Roma, Italy

²⁵ Henryk Niewodniczanski Institute of Nuclear Physics Polish Academy of Sciences, Kraków, Poland

²⁶ AGH - University of Science and Technology, Faculty of Physics and Applied Computer Science, Kraków, Poland

²⁷ National Center for Nuclear Research (NCBJ), Warsaw, Poland

²⁸ Horia Hulubei National Institute of Physics and Nuclear Engineering, Bucharest-Magurele, Romania

²⁹ Petersburg Nuclear Physics Institute (PNPI), Gatchina, Russia

³⁰ Institute of Theoretical and Experimental Physics (ITEP), Moscow, Russia

³¹ Institute of Nuclear Physics, Moscow State University (SINP MSU), Moscow, Russia

- ³² *Institute for Nuclear Research of the Russian Academy of Sciences (INR RAN), Moscow, Russia*
³³ *Budker Institute of Nuclear Physics (SB RAS) and Novosibirsk State University, Novosibirsk, Russia*
³⁴ *Institute for High Energy Physics (IHEP), Protvino, Russia*
³⁵ *Universitat de Barcelona, Barcelona, Spain*
³⁶ *Universidad de Santiago de Compostela, Santiago de Compostela, Spain*
³⁷ *European Organization for Nuclear Research (CERN), Geneva, Switzerland*
³⁸ *Ecole Polytechnique Fédérale de Lausanne (EPFL), Lausanne, Switzerland*
³⁹ *Physik-Institut, Universität Zürich, Zürich, Switzerland*
⁴⁰ *Nikhef National Institute for Subatomic Physics, Amsterdam, The Netherlands*
⁴¹ *Nikhef National Institute for Subatomic Physics and VU University Amsterdam, Amsterdam, The Netherlands*
⁴² *NSC Kharkiv Institute of Physics and Technology (NSC KIPT), Kharkiv, Ukraine*
⁴³ *Institute for Nuclear Research of the National Academy of Sciences (KINR), Kyiv, Ukraine*
⁴⁴ *University of Birmingham, Birmingham, United Kingdom*
⁴⁵ *H.H. Wills Physics Laboratory, University of Bristol, Bristol, United Kingdom*
⁴⁶ *Cavendish Laboratory, University of Cambridge, Cambridge, United Kingdom*
⁴⁷ *Department of Physics, University of Warwick, Coventry, United Kingdom*
⁴⁸ *STFC Rutherford Appleton Laboratory, Didcot, United Kingdom*
⁴⁹ *School of Physics and Astronomy, University of Edinburgh, Edinburgh, United Kingdom*
⁵⁰ *School of Physics and Astronomy, University of Glasgow, Glasgow, United Kingdom*
⁵¹ *Oliver Lodge Laboratory, University of Liverpool, Liverpool, United Kingdom*
⁵² *Imperial College London, London, United Kingdom*
⁵³ *School of Physics and Astronomy, University of Manchester, Manchester, United Kingdom*
⁵⁴ *Department of Physics, University of Oxford, Oxford, United Kingdom*
⁵⁵ *Massachusetts Institute of Technology, Cambridge, MA, United States*
⁵⁶ *University of Cincinnati, Cincinnati, OH, United States*
⁵⁷ *University of Maryland, College Park, MD, United States*
⁵⁸ *Syracuse University, Syracuse, NY, United States*
⁵⁹ *Pontifícia Universidade Católica do Rio de Janeiro (PUC-Rio), Rio de Janeiro, Brazil, associated to ²*
⁶⁰ *Institut für Physik, Universität Rostock, Rostock, Germany, associated to ¹¹*
⁶¹ *Celal Bayar University, Manisa, Turkey, associated to ³⁷*

- ^a *P.N. Lebedev Physical Institute, Russian Academy of Science (LPI RAS), Moscow, Russia*
^b *Università di Bari, Bari, Italy*
^c *Università di Bologna, Bologna, Italy*
^d *Università di Cagliari, Cagliari, Italy*
^e *Università di Ferrara, Ferrara, Italy*
^f *Università di Firenze, Firenze, Italy*
^g *Università di Urbino, Urbino, Italy*
^h *Università di Modena e Reggio Emilia, Modena, Italy*
ⁱ *Università di Genova, Genova, Italy*
^j *Università di Milano Bicocca, Milano, Italy*
^k *Università di Roma Tor Vergata, Roma, Italy*
^l *Università di Roma La Sapienza, Roma, Italy*
^m *Università della Basilicata, Potenza, Italy*
ⁿ *LIFAELS, La Salle, Universitat Ramon Llull, Barcelona, Spain*
^o *Hanoi University of Science, Hanoi, Viet Nam*
^p *Institute of Physics and Technology, Moscow, Russia*
^q *Università di Padova, Padova, Italy*
^r *Università di Pisa, Pisa, Italy*
^s *Scuola Normale Superiore, Pisa, Italy*

The asymmetry under simultaneous charge and parity transformation (CP violation) has driven the understanding of electroweak interactions since its discovery in the kaon system [1]. CP violation was subsequently discovered in the B^0 and B_s^0 systems [2–4]. Charmed mesons form the only neutral meson-antimeson system in which CP violation has yet to be observed unambiguously. This system is the only one in which mesons of up-type quarks participate in matter-antimatter transitions, a loop-level process in the Standard Model (SM). This charm mixing process has recently been observed for the first time unambiguously in single measurements [5–7]. The theoretical calculation of charm mixing and CP violation is challenging for the charm quark [8–12]. Significant enhancement of mixing or CP violation would be an indication of physics beyond the SM.

The mass eigenstates of the neutral charm meson system, $|D_{1,2}\rangle$, with masses $m_{1,2}$ and decay widths $\Gamma_{1,2}$, can be expressed as linear combinations of the flavour eigenstates, $|D^0\rangle$ and $|\bar{D}^0\rangle$, as $|D_{1,2}\rangle = p|D^0\rangle \pm q|\bar{D}^0\rangle$ with complex coefficients satisfying $|p|^2 + |q|^2 = 1$. This allows the definition of the mixing parameters $x \equiv 2(m_2 - m_1)/(\Gamma_1 + \Gamma_2)$ and $y \equiv (\Gamma_2 - \Gamma_1)/(\Gamma_1 + \Gamma_2)$.

Non-conservation of CP symmetry enters as a deviation from unity of λ_f , defined as

$$\lambda_f \equiv \frac{q\bar{A}_f}{pA_f} = -\eta_{CP} \left| \frac{q}{p} \right| \left| \frac{\bar{A}_f}{A_f} \right| e^{i\phi}, \quad (1)$$

where A_f (\bar{A}_f) is the amplitude for a D^0 (\bar{D}^0) meson decaying into a CP eigenstate f with eigenvalue η_{CP} , and ϕ is the CP -violating relative phase between q/p and \bar{A}_f/A_f . Direct CP violation occurs when the asymmetry $A_d \equiv (|A_f|^2 - |\bar{A}_f|^2)/(|A_f|^2 + |\bar{A}_f|^2)$ is different from zero. Indirect CP violation comprises non-zero CP asymmetry in mixing, $A_m \equiv (|q/p|^2 - |p/q|^2)/(|q/p|^2 + |p/q|^2)$ and CP violation through a non-zero phase ϕ . The phase convention of ϕ is chosen such that, in the limit of no CP violation, $CP|D^0\rangle = -|\bar{D}^0\rangle$. In this convention CP conservation leads to $\phi = 0$ and $|D_1\rangle$ being CP -odd.

The asymmetry of the inverse of effective lifetimes in decays of D^0 (\bar{D}^0) mesons into CP -even final states, $\hat{\Gamma}(\hat{\bar{\Gamma}})$, leads to the observable A_Γ defined as

$$A_\Gamma \equiv \frac{\hat{\Gamma} - \hat{\bar{\Gamma}}}{\hat{\Gamma} + \hat{\bar{\Gamma}}} \approx \eta_{CP} \left(\frac{A_m + A_d}{2} y \cos \phi - x \sin \phi \right). \quad (2)$$

This makes A_Γ a measurement of indirect CP violation, as the contributions from direct CP violation are measured to be small [13] compared to the current

precision [14]. Here, effective lifetimes refer to lifetimes measured using a single-exponential model in a specific decay mode. Currently available measurements of A_Γ [15, 16] are in agreement with no CP violation at the per mille level [13].

This Letter reports measurements of A_Γ in the CP -even final states K^-K^+ and $\pi^-\pi^+$ using 1.0 fb^{-1} of pp collisions at 7 TeV centre-of-mass energy at the LHC recorded with the LHCb detector in 2011. In the SM, the phase ϕ is final-state independent and thus measurements in the two final states are expected to yield the same results. At the level of precision of the measurements presented here, differences due to direct CP violation are negligible. However, contributions to ϕ from physics beyond the SM may lead to different results. Even small final-state differences in the phase, $\Delta\phi$, can lead to measurable effects in the observables of the order of $x\Delta\phi$, for sufficiently small phases ϕ in both final states [17]. In addition, the measurements of A_Γ in both final states is important to quantify the contribution of indirect CP violation to the observable ΔA_{CP} [18, 19].

The LHCb detector [20] is a single-arm forward spectrometer covering the pseudorapidity range $2 < \eta < 5$, designed for the study of particles containing b or c quarks. The polarity of the spectrometer dipole magnet was reversed periodically during the data taking period. The trigger [21] consists of a hardware stage, based on information from the calorimeter and muon systems, followed by a software stage, which performs a full event reconstruction. The software trigger applies two sequential selections. The first selection requires at least one track to have momentum transverse to the beamline, p_T , greater than 1.7 GeV/c and an impact parameter χ^2 , χ_{IP}^2 , greater than 16. The χ_{IP}^2 is defined as the difference in χ^2 of a given primary interaction vertex reconstructed with and without the considered track. This χ_{IP}^2 requirement introduces the largest effect on the observed decay-time distribution compared to other selection criteria. In the second selection this track is combined with a second track to form a candidate for a D^0 decay into two hadrons (charge conjugate states are included unless stated otherwise). The second track must have $p_T > 0.8\text{ GeV}/c$ and $\chi_{IP}^2 > 2$. The decay vertex is required to have a flight distance χ^2 per degree of freedom greater than 25 and the D^0 invariant mass, assuming kaons or pions as final state particles, has to lie within $50\text{ MeV}/c^2$ (or within $120\text{ MeV}/c^2$ for a trigger whose rate is scaled down by a factor of 10) around $1865\text{ MeV}/c^2$. The two-body system is required to point back to the pp interaction region.

The event selection applies a set of criteria that are

closely aligned to those applied at the trigger stage. The final-state particles have to match particle identification criteria to separate kaons from pions [22] according to their mass hypothesis and must not be identified as muons using combined information from the tracking and particle identification systems.

Flavour tagging is performed through the measurement of the charge of the pion in the decay $D^{*+} \rightarrow D^0 \pi^+$ (soft pion). Additional criteria are applied to the track quality of the soft pion as well as to the vertex quality of the D^{*+} meson. Using a fit constraining the soft pion to the pp interaction vertex, the invariant mass difference of the D^{*+} and D^0 candidates, Δm , is required to be less than $152 \text{ MeV}/c^2$.

About 10 % of the selected events have more than one candidate passing the selections, mostly due to one D^0 candidate being associated with several soft pions. One candidate per event is selected at random to reduce the background from randomly associated soft pions. The D^0 decay-time range is restricted to 0.25 ps to 10 ps such that there are sufficient amounts of data to ensure a stable fit.

The whole dataset is split into four subsets, identified by the magnet polarity, and two separate data-taking periods to account for known differences in the detector alignment and calibration. The smallest subset contains about 20% of the total data sample. Results of the four subsets are combined in a weighted average.

The selected events contain about 3.11×10^6 $D^0 \rightarrow K^- K^+$ and 1.03×10^6 $D^0 \rightarrow \pi^- \pi^+$ signal candidates, where the D^{*+} meson is produced directly in the pp collision, with purities of 93.6% and 91.2%, respectively, as measured in a region of two standard deviations of the signal peaks in D^0 mass, $m(hh)$ (with $h = K, \pi$), and Δm (an example fit projection is shown in Fig. 1).

The effective lifetimes are extracted by eight independent multivariate unbinned maximum likelihood fits to the four subsamples, separated by the D^0 flavour as determined by the charge of the soft pion. The fits are carried out in two stages, a fit to $m(hh)$ and Δm to extract the signal yield and a fit to the decay time and $\ln(\chi_{\text{IP}}^2)$ of the D^0 candidate to extract the effective lifetime. The first stage is used to distinguish the following candidate classes: correctly tagged signal candidates, which peak in both variables; correctly reconstructed D^0 candidates associated with a random soft pion (labelled “rnd. π_s ” in figures), which peak in $m(hh)$ but follow a threshold function in Δm ; and combinatorial background. The threshold functions are polynomials in $\sqrt{\Delta m - m_{\pi^+}}$. The signal peaks in $m(hh)$ and Δm are described by the sum of three Gaussian functions. For the $\pi^- \pi^+$ final state a power-law

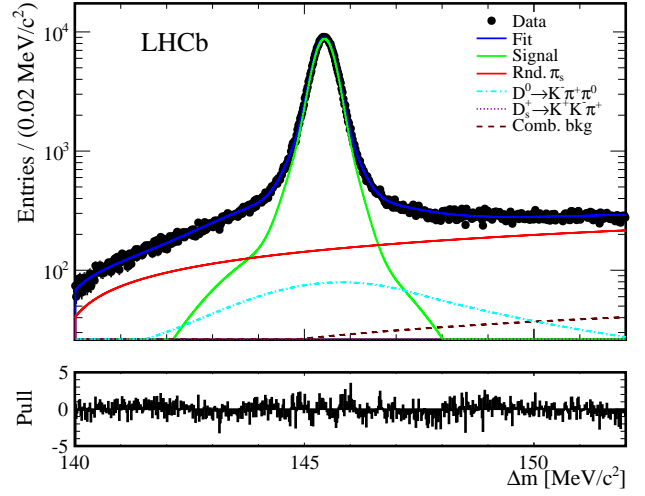


Figure 1: Fit of Δm for one of the eight subsets, containing the $\bar{D}^0 \rightarrow K^- K^+$ candidates with magnet polarity down for the earlier run period.

tail is added to the $m(hh)$ distribution to describe the radiative tail [23]. The combinatorial background is described by an exponential function in $m(hh)$ and a threshold function in Δm .

Partially reconstructed decays constitute additional background sources. The channels that give significant contributions are the decays $D^0 \rightarrow K^- \pi^+ \pi^0$, with the charged pion reconstructed as a kaon and the π^0 meson not reconstructed, and $D_s^+ \rightarrow K^- K^+ \pi^+$, with the pion not reconstructed. The former peaks broadly in Δm while the latter follows a threshold function and both are described by an exponential in $m(hh)$. Reflections due to incorrect mass assignment of the tracks are well separated in mass and are suppressed by particle identification and are not taken into account.

Charm mesons originating from long-lived b hadrons (secondary candidates) form a large background that cannot be separated in the mass fit. They do not come from the interaction point leading to a biased decay-time measurement. The flight distance of the b hadrons causes the D^0 candidates into which they decay to have large χ_{IP}^2 on average. This is therefore used as a separating variable.

Candidates for signal decays, where the D^{*+} is produced directly in the pp interaction, are modelled by an exponential function in decay time, whose decay constant determines the effective lifetime, and by a

modified χ^2 function in $\ln(\chi_{\text{IP}}^2)$ of the form

$$f(x) \equiv \begin{cases} e^{\alpha x - e^{\alpha(x-\mu)}} & x \leq \mu \\ e^{\alpha\mu + \beta(x-\mu) - e^{\beta(x-\mu)}} & x > \mu, \end{cases} \quad (3)$$

where all parameters are allowed to have a linear variation with decay time. The parameters α and β describe the left and right width of the distribution, respectively, and μ is the peak position. Secondary candidates are described by the convolution of two exponential probability density functions in decay time. Since there can be several sources of secondary candidates, the sum of two such convolutions is used with one of the decay constants shared, apart from the smaller $\pi^-\pi^+$ dataset where a single convolution is sufficient to describe the data. The $\ln(\chi_{\text{IP}}^2)$ distribution of secondary decays is also given by Eq. 3, however, the three parameters are replaced by functions of decay time

$$\alpha(t) = A + Bt + C \arctan(Dt), \quad (4)$$

and similarly for β and μ , where the parametrisations are motivated by studies on highly enriched samples of secondary decays.

The background from correctly reconstructed D^0 mesons associated to a random soft pion share the same $\ln(\chi_{\text{IP}}^2)$ shape as the signal. Other combinatorial backgrounds and partially reconstructed decays for the K^-K^+ final state are described by non-parametric distributions. The shapes are obtained by applying the *sPlot* technique [24] to the result of the $m(hh)$, Δm fit. Gaussian kernel density estimators are applied to create smooth distributions [25].

The detector resolution is accounted for by the convolution of a Gaussian function with the decay-time function. The Gaussian width is 50 fs, an effective value extracted from studies of $B \rightarrow J/\psi X$ decays [26], which has negligible effect on the measurement. Biases introduced by the selection criteria are accounted for through per-candidate acceptance functions which are determined in a data-driven way. The acceptance functions enter the fit in the normalisation of the decay-time parametrisations. The procedure for determination and application of these functions is described in detail in Refs. [15, 27]. Additional geometric detector acceptance effects are also included in the procedure. An example decay-time fit projection is shown in Fig. 2.

The fit has several regions where the model fails to describe the data accurately. The same deviations are observed in pseudo-experiment studies, and are reproduced in several independent parametrisations, indicating that the origin is related to the non-parametric

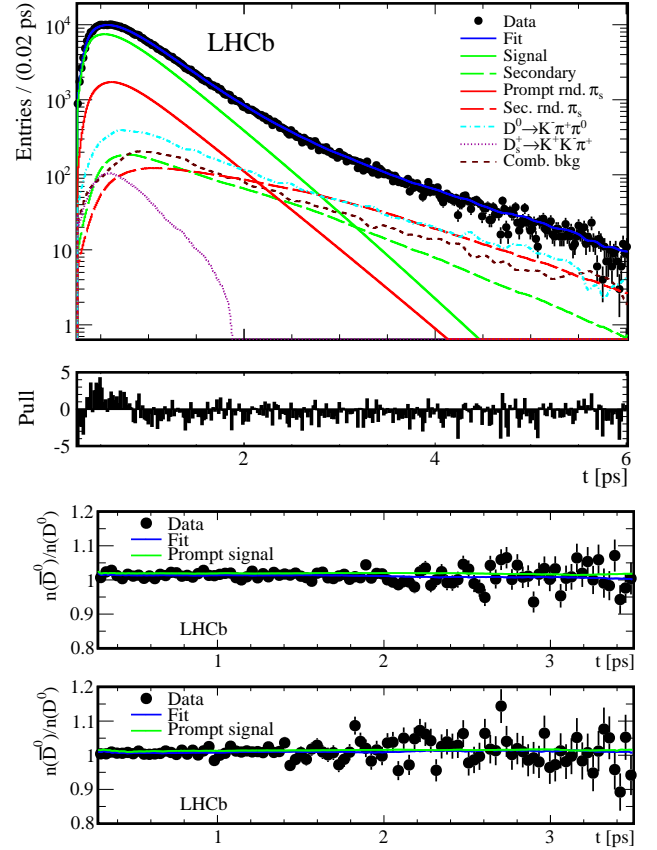


Figure 2: (Top) Fit of decay time to $\bar{D}^0 \rightarrow K^- K^+$ for candidates with magnet polarity down for the earlier run period and (middle and bottom) ratio of \bar{D}^0 to D^0 data and fit model for decays to $K^- K^+$ and $\pi^-\pi^+$ for all data, respectively.

treatment of backgrounds. They do not significantly affect the central value of A_Γ due to the low correlations between the effective lifetime and other fit parameters. The deviations are very similar for fits to D^0 and \bar{D}^0 samples leading to their cancellations in the final asymmetry calculations as shown in Fig. 2.

In addition to the nominal procedure an alternative method is used, in which the data are binned in equally-populated regions of the decay-time distribution and the ratio of \bar{D}^0 to D^0 yields calculated in each bin. This avoids the need to model the decay-time acceptance. The time dependence of this ratio, R , allows the calculation of A_Γ from a simple linear χ^2 minimisation, with

$$R(t) \approx \frac{N_{\bar{D}^0}}{N_{D^0}} \left(1 + \frac{2A_\Gamma}{\tau_{KK}} t \right) \frac{1 - e^{-\Delta t/\tau_{\bar{D}^0}}}{1 - e^{-\Delta t/\tau_{D^0}}}, \quad (5)$$

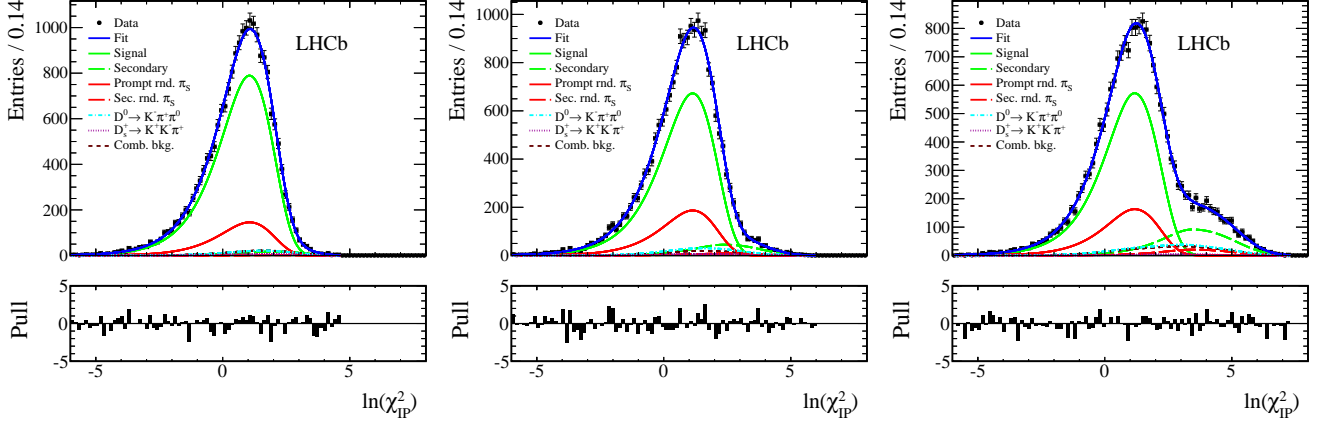


Figure 3: Fits of $\ln(\chi^2_{\text{IP}})$ for $\bar{D}^0 \rightarrow K^- K^+$ candidates for decay-time bins (left to right) $0.25 - 0.37$ ps, $0.74 - 0.78$ ps, and $1.55 - 1.80$ ps.

where $\tau_{KK} = \tau_{K\pi}/(1+y_{CP})$ is used as an external input based on current world averages [13, 28], $N_{\bar{D}^0}/N_{D^0}$ is the signal yield ratio integrated over all decay times and Δt is the bin width. The dependence on τ_{D^0} and $\tau_{\bar{D}^0}$ cancels in the extraction of A_Γ . For this method the prompt signal yields for each decay-time bin are extracted by simultaneous unbinned maximum likelihood fits to $m(hh)$, Δm , and $\ln(\chi^2_{\text{IP}})$. Each bin is chosen to contain about 4×10^4 candidates, leading to 118 and 40 bins for $K^- K^+$ and $\pi^- \pi^+$, respectively. In general, the binned fit uses similar parametrisations to the unbinned fit, though a few simplifications are required to account for the smaller sample size per bin. The evolution of the fit projections in $\ln(\chi^2_{\text{IP}})$ with decay time is shown in Fig. 3.

The fits for both methods are verified by randomising the flavour tags and checking that the results for A_Γ are in agreement with zero. Similarly, the measurement techniques for A_Γ are applied to the Cabibbo-favoured $K^- \pi^+$ final state for which they also yield results in agreement with zero. The unbinned fit is further checked by comparing the extracted lifetime using the $K^- \pi^+$ final state to the world average D^0 lifetime, (410.1 ± 1.5) fs [28]. The result of (412.88 ± 0.08) fs, where the uncertainty is only statistical, is found to be in reasonable agreement. If the full difference to the world average were taken as a relative systematic bias it would lead to an absolute bias of less than 10^{-4} on A_Γ . Large numbers of pseudo-experiments, with both zero and non-zero input values for A_Γ , are used to confirm the accuracy of the results and their uncertainties. Finally, dependencies on D^0 kinematics and flight direction, the selection at the hardware trigger

stage, and the track and vertex multiplicity, are found to be negligible.

The unbinned fit yields $A_\Gamma(KK) = (-0.35 \pm 0.62) \times 10^{-3}$ and $A_\Gamma(\pi\pi) = (0.33 \pm 1.06) \times 10^{-3}$, with statistical uncertainties only, and the binned fit yields $A_\Gamma(KK) = (0.50 \pm 0.65) \times 10^{-3}$ and $A_\Gamma(\pi\pi) = (0.85 \pm 1.22) \times 10^{-3}$. The results of the four subsets are found to be in agreement with each other for the nominal fit and the A_Γ measurements from the two methods yield consistent results.

The systematic uncertainties assessed are summarised in Table 1. The effect of shortcomings in the description of the partially reconstructed background component in the $K^- K^+$ final state is estimated by fixing the respective distributions to those obtained in fits to simulated data. The imperfect knowledge of the length scale of the vertex detector as well as decay-time resolution effects are found to be negligible. Potential inaccuracies in the description of combinatorial background and background from signal candidates originating from b -hadron decays are assessed through pseudo-experiments with varied background levels and varied generated distributions while leaving the fit model unchanged. The impact of imperfect treatment of background from D^0 candidates associated to random soft pions is evaluated by testing several fit configurations with fewer assumptions on the shape of this background.

The accuracy of the decay-time acceptance correction in the unbinned fit method is assessed by testing the sensitivity to artificial biases applied to the per-event acceptance functions. The overall systematic uncertainties of the two final states for the unbinned

Table 1: Systematic uncertainties, given as multiples of 10^{-3} . The first column for each final state refers to the unbinned fit method and the second column to the binned fit method.

Source	$A_{\Gamma}^{\text{unb}}(KK)$	$A_{\Gamma}^{\text{bin}}(KK)$	$A_{\Gamma}^{\text{unb}}(\pi\pi)$	$A_{\Gamma}^{\text{bin}}(\pi\pi)$
Partially reconstructed backgrounds	± 0.02	± 0.09	± 0.00	± 0.00
Charm from b decays	± 0.07	± 0.55	± 0.07	± 0.53
Other backgrounds	± 0.02	± 0.40	± 0.04	± 0.57
Acceptance function	± 0.09	—	± 0.11	—
Magnet polarity	—	± 0.58	—	± 0.82
Total syst. uncertainty	± 0.12	± 0.89	± 0.14	± 1.13

method have a correlation of 0.31.

A significant difference between results for the two magnet polarities is observed in the binned method. As this cannot be guaranteed to cancel, a systematic uncertainty is assigned. The unbinned method is not affected by this as it is not sensitive to the overall normalisation of the D^0 and \bar{D}^0 samples. In general the two methods are subject to different sets of systematic effects due to the different ways in which they extract the results. The systematic uncertainties for the binned method are larger due to the fact that the fits are performed independently in each decay-time bin. This can lead to instabilities in the behaviour of particular fit components with time, an effect which is minimised in the unbinned fit. The effects of such instabilities are determined by running simulated pseudo-experiments.

The use of the external input for τ_{KK} in the binned fit method does not yield a significant systematic uncertainty. A potential bias in this method due to inaccurate parametrisations of other background is tested by replacing the probability density functions by different models and a corresponding systematic uncertainty is assigned.

In summary, the CP -violating observable A_{Γ} is measured using the decays of neutral charm mesons into K^-K^+ and $\pi^-\pi^+$. The results of $A_{\Gamma}(KK) = (-0.35 \pm 0.62 \pm 0.12) \times 10^{-3}$ and $A_{\Gamma}(\pi\pi) = (0.33 \pm 1.06 \pm 0.14) \times 10^{-3}$, where the first uncertainties are statistical and the second are systematic, represent the world’s best measurements of these quantities. The result for the K^-K^+ final state is obtained based on an independent data set to the previous LHCb measurement [15], with which it agrees well. The results show no significant difference between the two final states and both results are in agreement with zero, thus indicating the absence of indirect CP violation at this level of precision.

Acknowledgements

We express our gratitude to our colleagues in the CERN accelerator departments for the excellent performance of the LHC. We thank the technical and administrative staff at the LHCb institutes. We acknowledge support from CERN and from the national agencies: CAPES, CNPq, FAPERJ and FINEP (Brazil); NSFC (China); CNRS/IN2P3 and Region Auvergne (France); BMBF, DFG, HGF and MPG (Germany); SFI (Ireland); INFN (Italy); FOM and NWO (The Netherlands); SCSR (Poland); MEN/IFA (Romania); MinES, Rosatom, RFBR and NRC “Kurchatov Institute” (Russia); MinECo, XuntaGal and GENCAT (Spain); SNSF and SER (Switzerland); NAS Ukraine (Ukraine); STFC (United Kingdom); NSF (USA). We also acknowledge the support received from the ERC under FP7. The Tier1 computing centres are supported by IN2P3 (France), KIT and BMBF (Germany), INFN (Italy), NWO and SURF (The Netherlands), PIC (Spain), GridPP (United Kingdom). We are thankful for the computing resources put at our disposal by Yandex LLC (Russia), as well as to the communities behind the multiple open source software packages on which we depend.

References

- [1] J. Christenson, J. Cronin, V. Fitch, and R. Turlay, *Evidence for the 2π decay of the K_2^0 meson*, Phys. Rev. Lett. **13** (1964) 138.
- [2] BaBar collaboration, B. Aubert *et al.*, *Observation of CP violation in the B^0 meson system*, Phys. Rev. Lett. **87** (2001) 091801, [arXiv:hep-ex/0107013](#).
- [3] Belle collaboration, K. Abe *et al.*, *Observation of large CP violation in the neutral B me-*

- son system, Phys. Rev. Lett. **87** (2001) 091802, arXiv:hep-ex/0107061.
- [4] LHCb collaboration, R. Aaij *et al.*, *First observation of CP violation in the decays of B_s^0 mesons*, Phys. Rev. Lett. **110** (2013) 221601, arXiv:1304.6173.
- [5] LHCb collaboration, R. Aaij *et al.*, *Observation of D^0 - \bar{D}^0 oscillations*, Phys. Rev. Lett. **110** (2013) 101802, arXiv:1211.1230.
- [6] CDF Collaboration, T. A. Aaltonen *et al.*, *Observation of D^0 - \bar{D}^0 mixing using the CDF II detector*, Phys. Rev. Lett. (2013) arXiv:1309.4078.
- [7] LHCb collaboration, R. Aaij *et al.*, *Measurement of D^0 - \bar{D}^0 mixing parameters and search for CP violation using $D^0 \rightarrow K^+\pi^-$ decays*, arXiv:1309.6534, submitted to Phys. Rev. Lett.
- [8] M. Bobrowski, A. Lenz, J. Riedl, and J. Rohrwild, *How large can the SM contribution to CP violation in D^0 - \bar{D}^0 mixing be?*, JHEP **03** (2010) 009, arXiv:1002.4794.
- [9] H. Georgi, *D - \bar{D} mixing in heavy quark effective field theory*, Phys. Lett. **B297** (1992) 353, arXiv:hep-ph/9209291.
- [10] T. Ohl, G. Ricciardi, and E. H. Simmons, *D - \bar{D} mixing in heavy quark effective field theory: the sequel*, Nucl. Phys. **B403** (1993) 605, arXiv:hep-ph/9301212.
- [11] I. I. Bigi and N. G. Uraltsev, *D^0 - \bar{D}^0 oscillations as a probe of quark hadron duality*, Nucl. Phys. **B592** (2001) 92, arXiv:hep-ph/0005089.
- [12] A. Lenz and T. Rauh, *D meson lifetimes within the Heavy Quark Expansion*, arXiv:1305.3588.
- [13] Heavy Flavor Averaging Group, Y. Amhis *et al.*, *Averages of b -hadron, c -hadron, and τ -lepton properties as of early 2012*, arXiv:1207.1158, updated results and plots available at <http://www.slac.stanford.edu/xorg/hfag/>.
- [14] M. Gersabeck *et al.*, *On the interplay of direct and indirect CP violation in the charm sector*, J. Phys. **G39** (2012) 045005, arXiv:1111.6515.
- [15] LHCb collaboration, R. Aaij *et al.*, *Measurement of mixing and CP violation parameters in two-body charm decays*, JHEP **04** (2012) 129, arXiv:1112.4698.
- [16] BaBar collaboration, J. P. Lees *et al.*, *Measurement of D^0 - \bar{D}^0 mixing and CP violation in two-body D^0 decays*, Phys. Rev. **D87** (2013) 012004, arXiv:1209.3896.
- [17] A. L. Kagan and M. D. Sokoloff, *On indirect CP violation and implications for D^0 - \bar{D}^0 and B_s^0 - \bar{B}_s^0 mixing*, Phys. Rev. **D80** (2009) 076008, arXiv:0907.3917.
- [18] LHCb collaboration, R. Aaij *et al.*, *Evidence for CP violation in time-integrated $D^0 \rightarrow h^-h^+$ decay rates*, Phys. Rev. Lett. **108** (2012) 111602, arXiv:1112.0938.
- [19] LHCb collaboration, R. Aaij *et al.*, *Search for direct CP violation in $D^0 \rightarrow h^-h^+$ modes using semileptonic B decays*, Phys. Lett. **B723** (2013) 33, arXiv:1303.2614.
- [20] LHCb collaboration, A. A. Alves Jr. *et al.*, *The LHCb detector at the LHC*, JINST **3** (2008) S08005.
- [21] R. Aaij *et al.*, *The LHCb trigger and its performance in 2011*, JINST **8** (2013) P04022, arXiv:1211.3055.
- [22] M. Adinolfi *et al.*, *Performance of the LHCb RICH detector at the LHC*, Eur. Phys. J. **C73** (2013) 2431, arXiv:1211.6759.
- [23] T. Skwarnicki, *A study of the radiative cascade transitions between the Upsilon-prime and Upsilon resonances*, PhD thesis, Institute of Nuclear Physics, Krakow, 1986, DESY-F31-86-02.
- [24] M. Pivk and F. R. Le Diberder, *sPlot: a statistical tool to unfold data distributions*, Nucl. Instrum. Meth. **A555** (2005) 356, arXiv:physics/0402083.
- [25] D. Scott, *Multivariate density estimation: theory, practice, and visualization*, John Wiley and Sons, Inc, 1992.
- [26] LHCb collaboration, R. Aaij *et al.*, *Measurement of the CP-violating phase ϕ_s in the decay $B_s^0 \rightarrow J/\psi\phi$* , Phys. Rev. Lett. **108** (2012) 101803, arXiv:1112.3183.
- [27] V. Gligorov *et al.*, *Swimming: A data driven acceptance correction algorithm*, J. Phys. Conf. Ser. **396** (2012) 022016.

- [28] Particle Data Group, J. Beringer *et al.*, *Review of particle physics*, Phys. Rev. **D86** (2012) 010001, and 2013 partial update for the 2014 edition.